NEBULAR COMPLEX IN THE REGION OF CAS OB2 ASSOCIATION; RING NEBULA SH157

T. A. LOZINSKAYA, T. G. SITNIK, and A. I. LOMOVSKII

Sternberg State Astronomical Institute, Moscow, U.S.S.R.

Abstract. This paper presents the results of monochromatic [O III], [N II], and [S II] observations of ring nebula Sh157 around the star (WR + B0III) HD 219460 belonging to the Ba 3 cluster. A stratification of radiation typical for photoionization excitation has been revealed. The observations suggest that the Sh157 ring structure may arise as a result of the HD 219460 stellar wind blowing the surrounding H II region, and the bubble age is found to be $t \simeq (2 - 5) \times 10^5$ yr. Three outer envelopes have been distinguished: a weaker extended emission shell apparently blown out by the wind from B-stars of the Ba 3 cluster, and two dust shells which are likely to be associated with NGC 7510 and Cas OB2. The paper is also concerned with the discussion of young star aggregates Ba 3, NGC 7510, Cas OB1, OB2, OB4, OB5, OB7, and Cep OBI and the associated H II regions, shells and supershells of gas and dust, molecular clouds, and supernova remnants which may be probable members of a single giant stellar complex where the star formation process is in progress.

Introduction

The present paper covers the results of the observations of the ring-nebula Sh157 (Sharpless, 1959) around the open cluster Ba 3 (Ma 50) and discusses the problem of whether Ba 3, Sh157 and a number of young stellar clusters and associated dust and emission shells, H II regions and molecular clouds in the Perseus spiral arm could belong to a single star complex.

The accomplished monochromatic observations of the nebula Sh157 continue our studies of stratification of radiation in the lines of high- and low-ionization stage in nebulae of different origin (see Sitnik and Toropova, 1982; Sitnik *et al.*, 1983; Lozinskaya *et al.*, 1984, 1985). The northern part of Sh157 or Simeiz 274 (Gaze and Shain, 1955) – the object denoted as SG 13 in the catalogue of Shain and Gaze (1951) is a thin shell around the cluster Ba 3 (Grubissisch, 1965) or Ma 50 (Markarian, 1951). The cluster includes the Wolf–Rayet star with B0 III companion HD 219460; therefore, the ring-shaped structure of the nebula apparently results from the action of a strong stellar wind sweeping the surrounding gas. The southern part of Sh157, i.e., SG 14, more diffuse and featureless, is apt to be excited by some more OB stars not belonging to the cluster Ba 3.

The nebula Sh157 and the cluster Ba 3 are located in a densely-populated sector of the sky (see Figure 1). Located here within an area of $108 \leq l \leq 115°$, $-2.5 \leq b \leq 2°$ in the line-of-sight are three more galactic open clusters (NGC 7510, Ba 2, NGC 7654) and association Cas OB2 comprising some 20 B giants and supergiants, two O_f stars, and, probably, WR star.

Eleven H II regions can be observed in the region of interest both in optical and in radio frequency ranges, including two bright ring nebulae around a source of strong
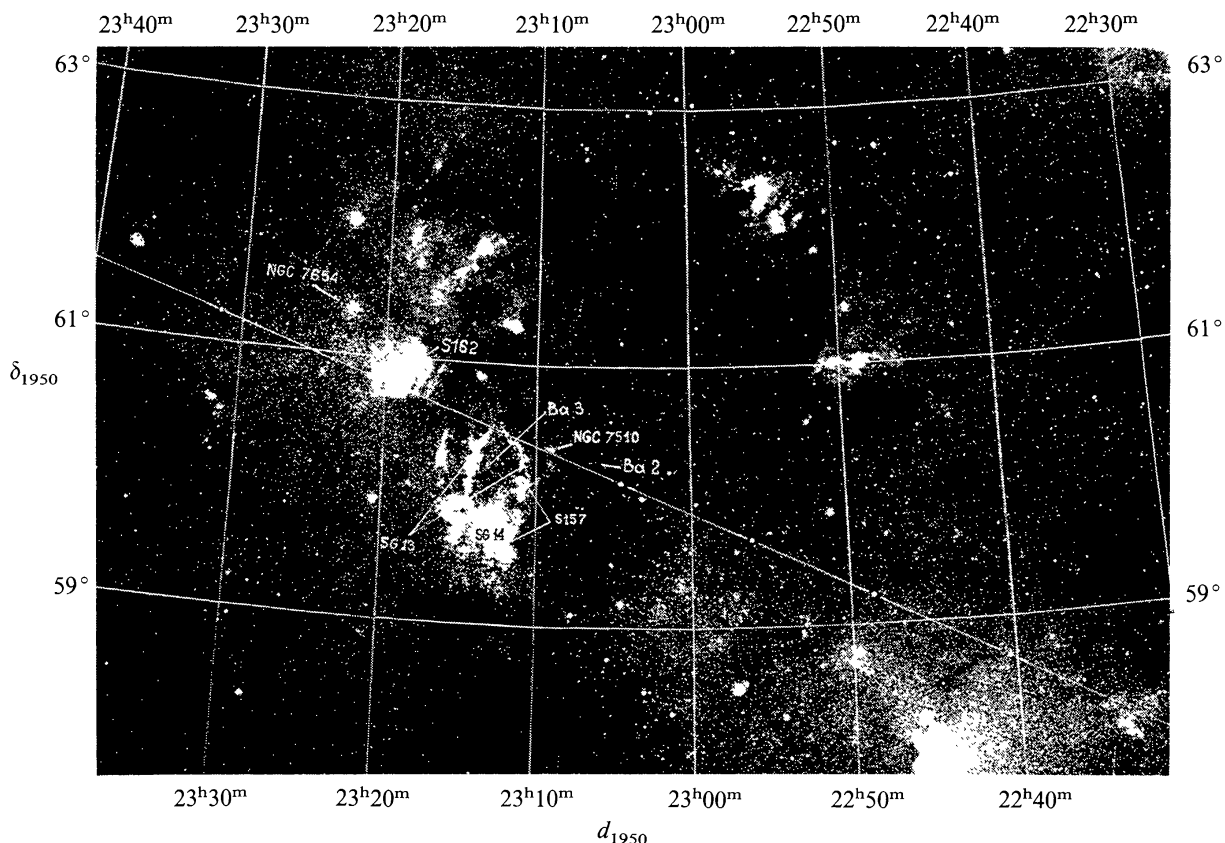
Fig. 1.   Photograph of sky sector under consideration (mosaic of red cards of the *Palomar Sky Atlas*). The galactic plane is shown by dot-and-dash line.

stellar wind, viz., nebula Sh157 under consideration and the shell NGC 7635 around the star O_f BD $60°2522$. (The monochromatic observations of the latter were carried out in similar way by Lomovskii and Klement'eva, 1985). Located in the same area are numerous dust and molecular clouds observable both in radiation and in absorption in the lines CO, H I, H_2, H_2CO, $C_{427\alpha}$–$C_{732\alpha}$, etc., in the radio frequency range. In the close neighbourhood there are a few old supernova remnants and a youngest galactic supernova remnant Cas A all studied comprehensively in the radio- as well as in the optical and X-ray spectral ranges. Several compact sources – probable protostellar objects – are observed here in the IR range. The fact that the process of star formation is being in progress is attested to by masers OH–H_2O discovered in the dense clouds.

The observations of the nebula Sh157 and the data reductions will be discussed below in Sections 1 and 2. Section 3 of the paper is devoted to analysis of radial velocities, kinematic, and photometric distances to the stars, stellar aggregates, nebulae and molecular clouds in the region of interest. Of all the variety of the projected objects the Perseus arm population has been selected, which the nebula Sh157 belongs to. In addition to the bright ring nebula Sh157 whose nature is discussed below in Section 4, we have succeeded in distinguishing three less pronounced gas-dust shells, namely: weak external H II shell blown out most likely by the wind of B stars of the cluster Ba 3, and dust shells around NGC 7510 and Cas OB2 (Sections 4 and 5). Section 6 sets forth

a conclusion about probable genetic relationship of the relevant stellar aggregates, gas-dust envelopes, H II regions, molecular clouds, and supernova remnants drawn on the basis of consideration of their morphology, mutual separation distances and ages. In all likelihood, observed in the Perseus arm is a single giant star complex incorporating the associations Cas OB1, OB2, OB4, OB5, OB7, Ceph OB1, wherein the star formation process is still in progress.

1. Observation of the Nebula Sh157

The spectral and monochromatic observations of the nebula Sh157 (SG 13 + SG 14) were performed in autumn of 1984.

1.1. The monochromatic photographs in the lines [O III] 5007 Å, [N II] 6584 Å, and [S II] 6717 + 6731 Å were taken by the use of a focal reducing camera f : 1 and a contact image converter, type FCT1. The images from the converter screen were taken on the Kodak 103 aG photoemulsion. The parameters of the used interference filters, the number of the obtained photographs and the exposure time are presented in Table I.

TABLE I

Spectral lines	Parameters of filters			Exposure time (min.)	Number of photographs
	I_{max} (%)	λ_{max} (Å)	$\Delta\lambda_{1/2}$ (Å)		
[O III]	50	5007	30	15	33
[N II]	67	6583	20	12	35
[S II]	50	6723	40	15	21

The monochromatic observations were performed at the Cassegrain focus of the 125-cm and 60-cm reflectors at the Southern station of the Sternberg State Astronomical Institute, the angular resolution being 5–6″ and 15–17″, respectively.

The photo-mosaics of the H II region Sh157 in the lines [O III] and [N II] derived with the 60-cm reflector are illustrated in Figure 2. Figure 3 demonstrates the mosaic photographs of the eastern part of the shell SG 13 (let it be denoted by SG 13 E), particularly bright in the lines [O III] and [N II], obtained with the 125-cm reflector. With a view to revealing the stratification of emission in the high- and low-excitation lines, the photographs of this most interesting region of the nebula were reduced by the photographic euidensitometric method. (The description of the method as applied to the small-scale photographs taken from the electron image converter screen can be found in the works of Sitnik and Toropova, 1982, or Lozinskaya et al., 1986.)

As a result of the reduction the systems of isophotes of some sections of the nebula were derived in [O III], [N II], and [S II] lines. Because the angular size of SG 13 E exceeds the field of view of the system (10′ at the focus of the 125-cm reflector) the
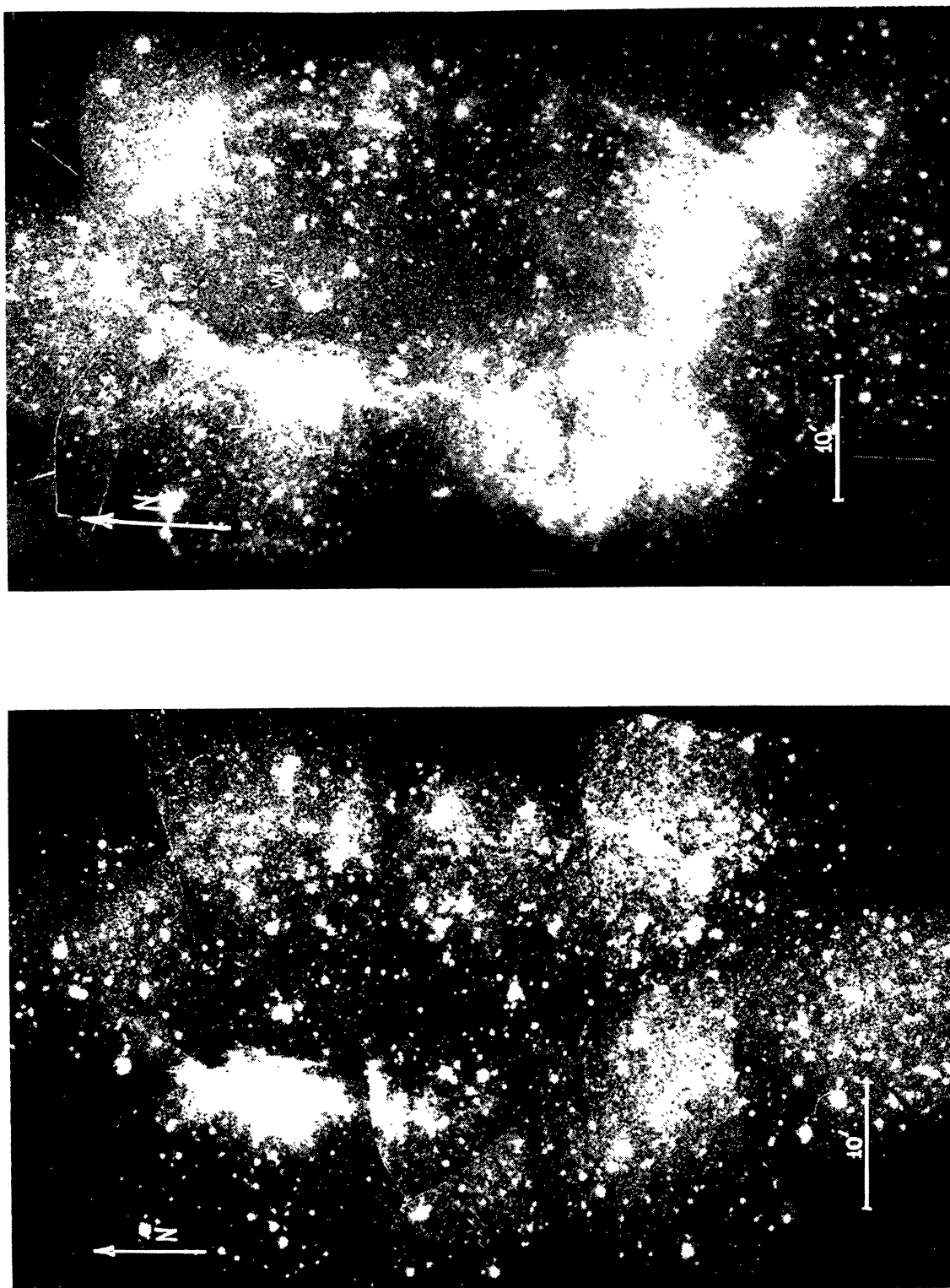
T. A. LOZINSKAYA ET AL.

Fig. 2. Photomosaic of the nebula Sh157 in [OIII] (a) and [NII] (b) lines; composition of negatives obtained with the 60-cm reflector. Several reference stars are shown by figures.
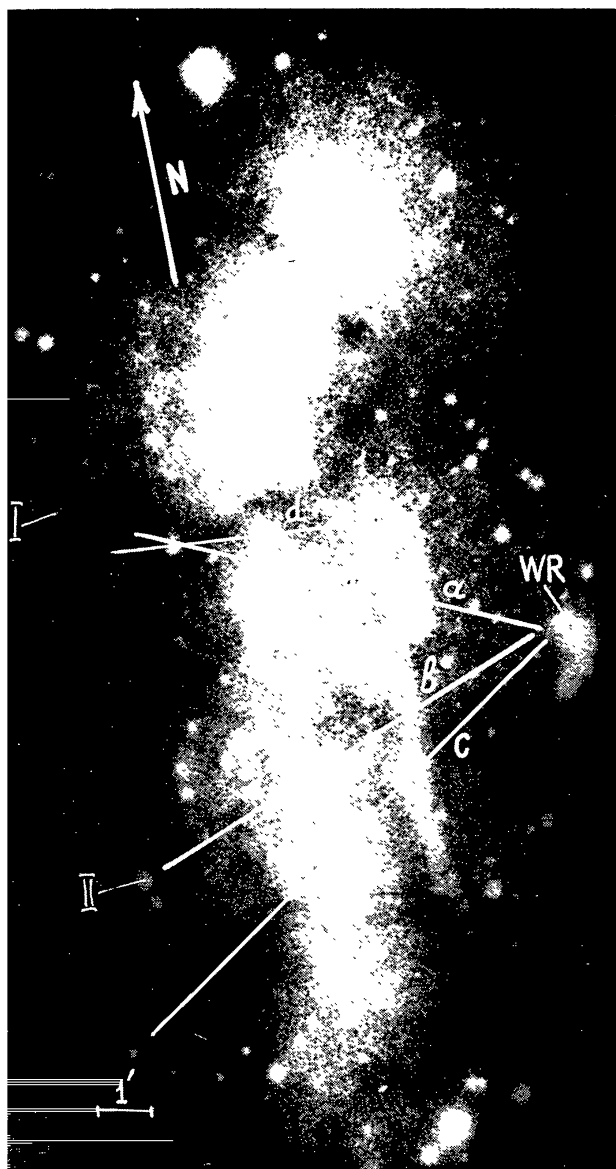
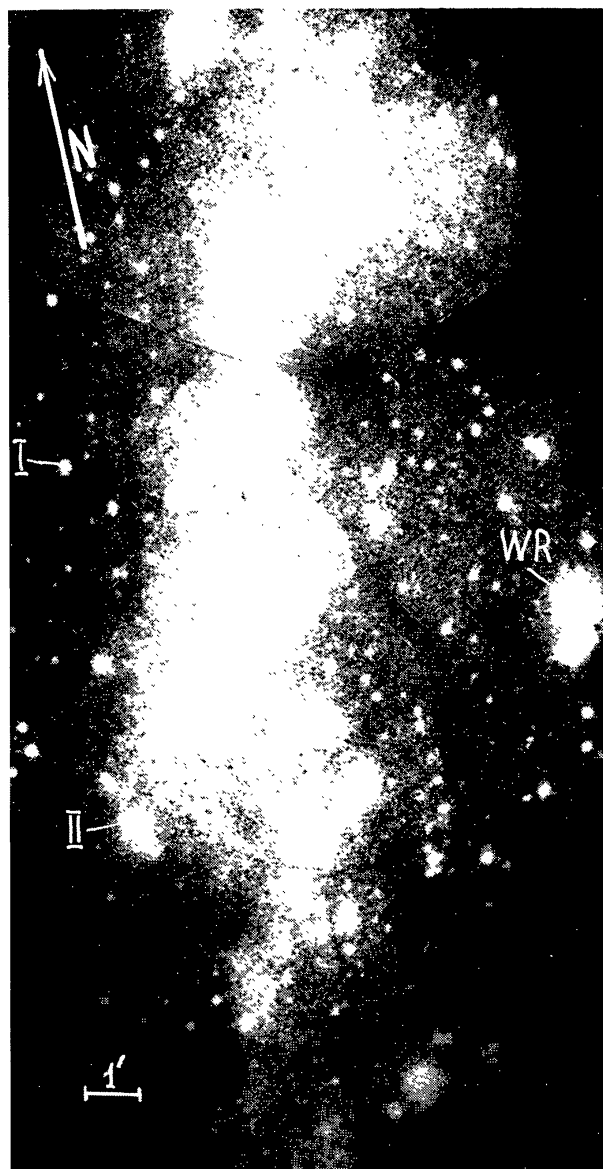Fig. 3a.   Fig. 3b.

Fig. 3.   Photo-mosaic of the nebula SG 13 E in [O III] (a), [N II] (b), and [S II] (c) lines; composition of negatives obtained with the 125-cm reflector. Several reference stars are marked and the direction of microphotometric scans are shown. The scan '*d*' coincides with the spectrograph slit orientation.

isophotes of the entire region as a whole were obtained by aligning of isophotes of several negatives so as to have them brought in coincidence on the overlapping sections. Such aligned isophotes are shown in Figure 4. The intensities are expressed in relative units different for each line. Their values are given in Figure 4. The error in determination of the intensity of the individual isophotes does not exceed 20%, the accuracy of localization of the aligned isophotes being no worse than $\simeq 8''$. (The isophotes were calibrated on the basis of microphotometric scans of the monochromatic photographs.)
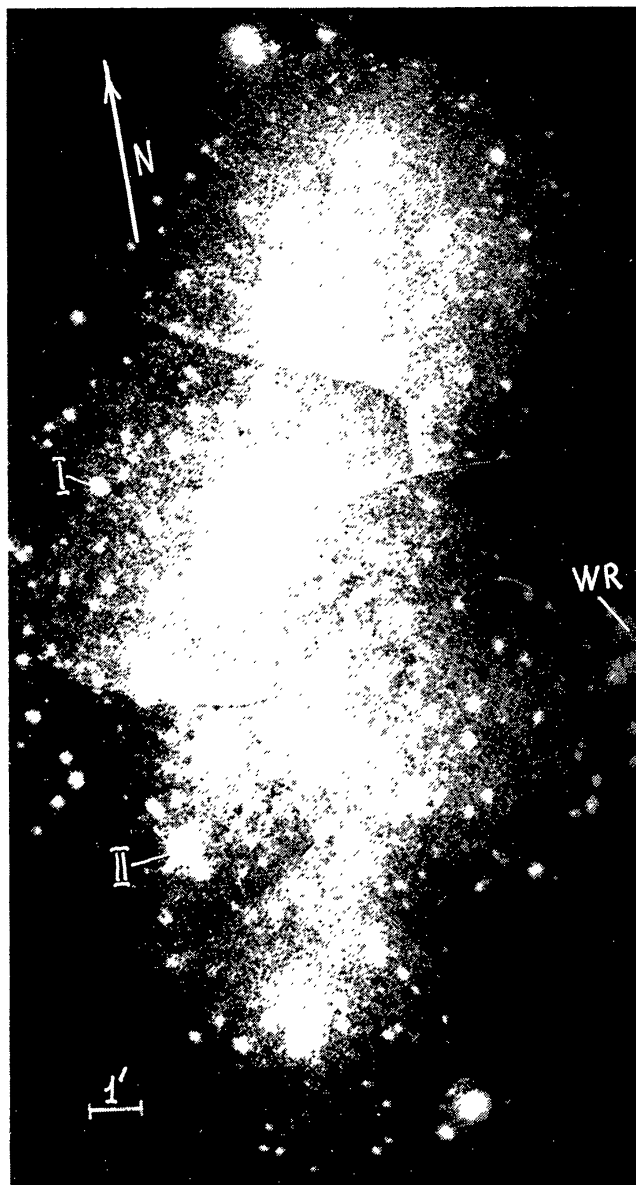
Fig. 3c.

The variation of the monochromatic intensities against the distance from the WR star (in the visual plane) is given in Figures 5(a–c). The positions of the scans on the nebula image are marked in Figure 3(a).

1.2. SPECTRAL OBSERVATIONS

The spectrogram of the bright region of the SG13 E was derived by Arkhipova and Lomovskii using a diffraction spectrograph with a single-stage fibre-optics electron image converter at the Cassegrain focus of the 125-cm reflector. The linear dispersion amounted to $100 \, \text{Å mm}^{-1}$, with the angular resolution being equal to $2-3''$. The localization of the spectrographs slit on the nebula is shown in Figure 3(a). The spectrogram was reduced by using the standard spectrophotometric method.

TABLE II

	$I([O\,III])/$ $I(H\alpha)$	$I(3729)/$ $I(3726)$	$I([S\,II])/$ $I(H\alpha)$	$I([N\,II])/$ $I(H\alpha)$	$I(6717)/$ $I(6732)$	n_e (cm^{-3})	References
S157 (SG 13 E)			0.11–0.25	0.15–0.38	1.21–1.4	50–270	Present paper
S157A	1.3						Chopinet and Lortet-Zuckerman (1976)
S157A			0.8	0.4[a]		$\geq 10^3$	Glushkov et al. (1972)
S157A		1.22				10^3	Deharveng (1974)

[a] $I(6584)/I(H\alpha)$.

Table II contains the relative intensities and the electron density derived on basis of our observations and the results obtained by other authors. The electron density was determined by the ratio of I_{6717}/I_{6732}. For estimating the density use was made of the calculations by Nosov (1979) for $T_e = 10^4$ K.

2. Reductions of the Sh157 Observations

2.1. Emission spectrum of SG 13 E region

As will be apparent from Table II, Hα line is found to be the brightest one in the spectrum of the nebula under consideration. The relative intensities of lines $I([S\,II])/I(H\alpha) = 0.11$–0.25 bear witness to a photoionization excitation. (The specific values of the intensity observed in old supernova remnants, where emission is completely determined by de-excitation of cooling gas after passing the shock wave, amount to $I([S\,II])/I(H\alpha) \simeq 1$.)

The electron density estimated by line [S II] is $\bar{n}_e \sim 100$–150 cm^{-3} on average for the nebula and $n_e \simeq 300$ cm^{-3} in the most luminous knots and filaments.

Taking account of the shell structure with pronounced dense condensations the foregoing values are in good agreement with the mean density of $n_e \sim 60$–70 cm^{-3} derived on the basis of the integrated Hα-brightness of SG 13 (Gershberg and Metik, 1960) on the assumption of a homogeneous distribution of the density (with a correction introduced for the accepted distance of $r \sim 2.5$ kpc).

2.2. Morphology of the nebula Sh157

When comparing the obtained large-scale images of the nebula Sh157 in the high- and low-excitation lines, it is found natural to come to the following conclusion.

The radiation is concentrated in a thin ($\Delta R/R \simeq 0.1$–0.2) shell of approximately regular elliptic shape with a knotty filamentary structure. The brightness distribution
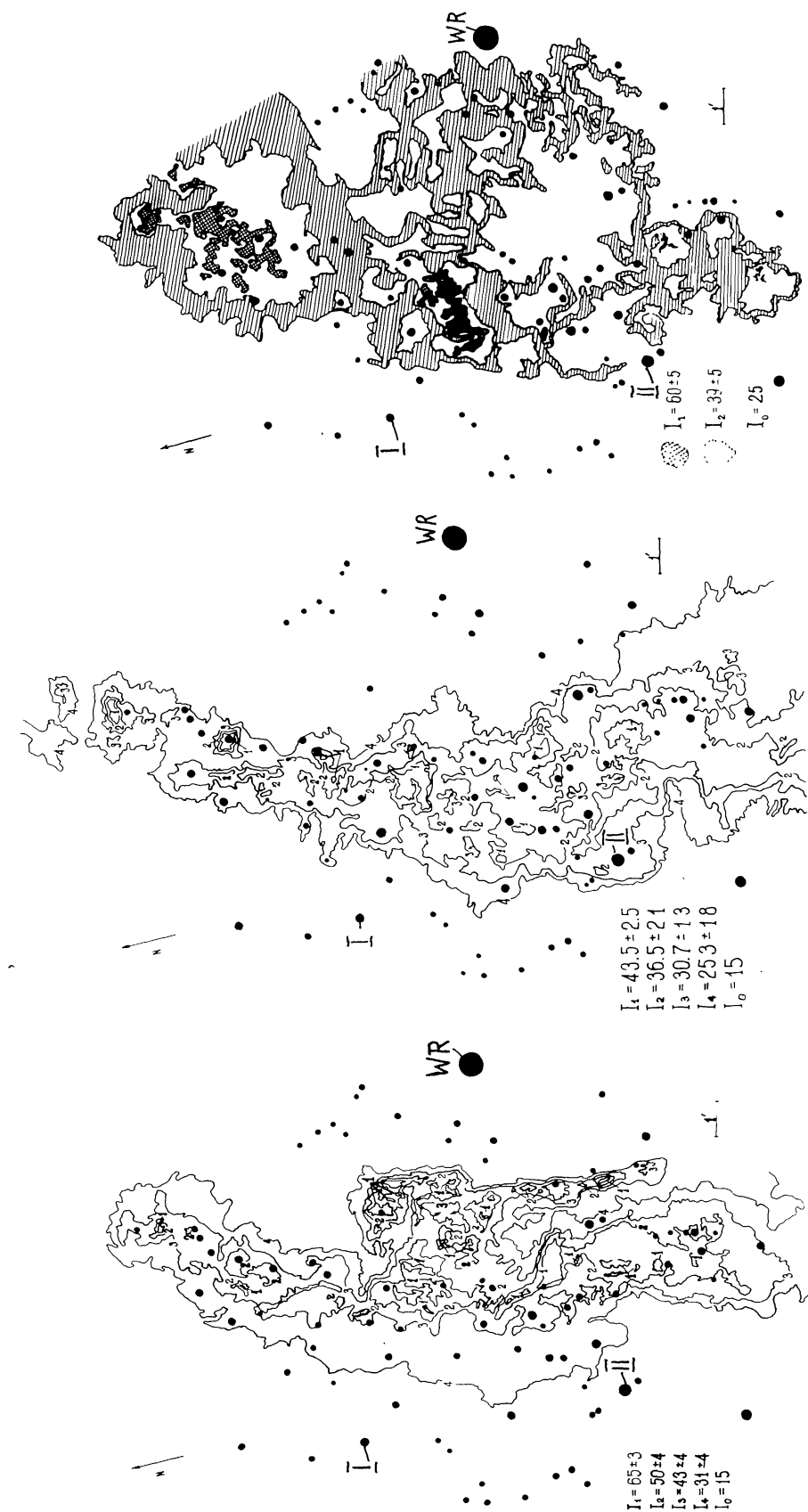
Fig. 4. System of isophotes of the region SG 13 E in [O III] (a), [N II] (b), and [S II] (c) lines obtained by the method of photographic equidensitometry. Isophotes are calibrated in relative units different for each line; their values are given in the left-down corner. Index 'o' corresponds to the intensity of the background radiation beyond the boundary of the nebula. The white regions between I_1 and I_2 on Figure 4(c) corresponds to $I = 50 \pm 10$.

over the shell in the lines [N II], Hα, and [S II] features a better homogeneity than in [O III] line. The bright region SG 13 E – the envelope part closest to the Ba 3 cluster – sharply stands out in line [O III]. The brightness in the low-excitation lines is also more intense here, however the contrast seems to be not too great. The southern area of Sh157 (SG 14) features a more diffuse morphology as compared to the northern area (SG 13). The ring-like structure of the nebula is seen more distinctly in the line [O III]. The shell as a whole does not show a prominent fine filamentary structure peculiar to some old supernova remnants or to bubbles blown by the wind of the stars WR and O_f, exception being an extremely fine rectilinear filament in the inner part of SG 13 E, brightly exhibited in the line [O III].

2.3. STRATIFICATION OF EMISSION

A thorough comparison of the monochromatic images enables the emission stratification to be revealed in lines [O III] relative [N II] and [S II]. In the central part of the region SG 13 E the whole system of [O III]-isophotes is displaced to the shell's center as compared with the [N II]-isophotes (Figure 4). The bright [O III] filament is located approximately by 2′ (1.4 pc) nearer to the star WR than the brightest details in the lines [N II] and [S II]. No mutual shift between the regions emitting in the lines [N II] and [S II] is noted because of diffuse character of the [S II] emission.

3. Estimate of Distances and General Structure of Galactic Disc in the Sector of the Sky $108 \leq l \leq 115°$

The problem of physical relationship between different components of stellar population and interstellar medium in the region of interest, i.e., whether they are members of a single giant stellar and molecular complex or just represent an accidental projection of distant-spaced formations, rests on accuracy of determination of the distances. Uncertainty of the kinematic distances at these galactic longitudes is more essential than in other directions because of large-scale peculiar motions in the Cassiopeia–Perseus arm (Humphreys, 1970).

The probable error in kinematic distances derived in terms of the Schmidt's model of circular motion reaches $\simeq 1$ kpc and over. That is why we shall relay hereinafter primarily upon photometric distances to the exciting stars, whereas the measurements of the radial velocity of the emission nebulae and absorbing clouds will be used merely for drawing conclusions about similarity or difference of the distances rather than for estimating its value.

A 'lucky chance' is the localization of the supernova remnant Cas A in this area of the sky. The distance to this remnant $R = 2.8$ kpc was derived from comparison of the radial velocities and the proper motions of a few hundreds filaments (Kamper and Van den Bergh, 1983; Sakhibov, 1980; the associated references *ibid.*). This is the most reliable of the known methods of estimate of distance to nebulae, and we use the supernova remnant Cas A as a calibrator for fitting the radial velocity to the distance at this galactic longitude.

TABLE III

Object	l^{II}, b^{II}	α, δ (1950)	θ	E_{B-V}	A_V	$(m-M)_0$	V_{LSR} km s^{-1}	r (kpc) Photometric	r (kpc) Kinematic	References
1	2	3	4	5	6	7	8	9	10	11
Associations, clusters, stars										
Cas OB2	112 + 2.5	23h20m 61°	4° × 3°		1m8–4m3	12m1		2.6		1
Ba 2	110.6 + 0.1	23h06m7 60°14'	7'	0.73	2.26	10.08		1.04		2
NGC 7510	111.0 + 0.0	23h09m4 +60°18'	6'				−49 (HI) −49 (stars)			3 3
				1m1	3.3	12.3		2.88		4, 5
				0.89		12.6		3.0		6, 7
				1.16	3.59	12.48		3.14		2
HD 219460 (WN 4.5)	111.33 − 0.24	23h13m02s 60°10'40"		0.95	2.85	12.0		2.5		8
				0.73	2.99	11.3		1.85		9
Ba 3 (Ma 50)	111.4 − 0.3	23h13m2 60°10'	5'	0.86	2.58	11.72		2.25		10, 5, 7
				0.94	2.8	12.0	−71 (stars)	2.5		8
				0.75	2.33	11.42		1.9		2
NGC 7654	112.8 + 0.5	23h22m0 61°19'	13'	0.49	1.53	10.42		1.21		2
BD + 60°2522 O$_f$	112.2 + 0.2	23h18m5 +60°55'			2.19	–		2.8		11
Emission nebulae										
S146	108.2 + 0.59	22h47m5 +59°39'	2'				−50 (CO)			12
S147	108.27 − 1.07	22h53m6 +58°12'	2'				−57 (CO)			12

Source	l, b	R.A. Dec.	Size	mag	Velocity (line)			Ref.
S148	108.35 − 1.05	22^{h}54^m.2 +58°16′	2′		−53 (CO)	5.5 ± 1.8		12
S149	108.38 − 1.05	22^{h}54^m.3 +58°17′	1′		−53 (CO)	5.4 ± 1.7		12
S152	108.77 − 0.95	22^{h}56^m.7 58°32′	2′		−50 (CO)	3.6 ± 1.1		12
					−36(Hα)		3.04 ± 0.39	13, 14
S153	108.8 − 1.02	22^{h}57^m.2 58°28′	5′	13^m.62	−51 (CO)	4.0 ± 1.3		13
					−55 (Hα)		4.57 ± 0.38	14
					−48 (Hα)		4.17	13
S154	109.0 + 1.6	22^{h}49^m.7 60°53′		11^m.2	−12 (Hα)		1.22	13, 14
					−12 (CO)	1.4 ± 0.4		12
S156	110.11 + 0.06	23^{h}03^m.1 59°59′	2′		−51 (CO)	6.4 ± 2.0		12
					−51 (Hα)		4.26	13
					−54 (OH)			15
							4.10 ± 0.38	14
S155	110.2 + 2.6	22^{h}55^m 62°19′		9^m.3	−16 (Hα)		1.49	13
							1.38 ± 0.42	14
					−10 (CO)	0.72		12
						0.73 ± 0.12		
S157 (SG 13) around Ba 3 and HD 219460	111.2 − 0.5	23^{h}12^m.6 59°55′			−53, −33, −55, −48 (Hα)			16
					−43 (CO)	2.5 ± 0.4		12, 17
					−43 (H$_{166α}$)			18
S157 A	111.3 − 0.7	23^{h}13^m.9 59°46′	3′ × 2′		−46 (Hα)			19
					−41 (Hα)			20
					−38 (Hα)		3.2	13
					−43 (CO)	2.5 ± 0.4		12, 17
S158 (NGC 7538)	111.55 + 0.82	23^{h}11^m.5 61°14′	10′	12^m.47	−60 (Hα)	3.1	4.75 ± 0.38	14
					−40 (Hα)			20
					−51 (Hα)		4.23	13
					−54 (Hα)			21
					−56 (CO)	2.8 ± 0.9		12
					−61 (H$_{109α}$)			22
					−74, − 60,			
					−53 (OH)			15
					−57 (HCN)			23
					−64 − −54 (H$_2$O)			23

Table III (continued)

Object	l^{II}, b^{II}	α, δ (1950)	θ	E_{B-V}	A_V	$(m-M)_0$	V_{LSR} km s^{-1}	r (kpc) Photometric	Kinematic	References
1	2	3	4	5	6	7	8	9	10	11
S159	111.64 + 0.37	23^{h}13^{m}6 / 60°51'	7'				−56 (CO)			12
S161 A	111.8 + 1.07	23^{h}13^{m}3 / 61°35'					−10 (CO)	2.8 ± 0.9		12
S161 B	111.8 + 1.07	23^{h}13^{m}3 / 61°35'	55'				−52 (CO)	2.8 ± 0.9		12
S162 (NGC 7635) around BD+60°2522	112.22 + 0.23	23^{h}18^{m}5 / 60°55'	40'	0″73		12^{m}0	−45 (Hα)	2.5		24
							−49 (Hα)	2.3	3.61 ± 0.37	14, 20
							−43 (Hα)		3.5	21
							−45 (CO)	3.5 ± 1.1		13
										12
S163	113.54 − 0.65	23^{h}31^{m}0 / 60°30'	10'			12^{m}39	−45 (CO)	2.3 ± 0.7	3.35 ± 0.37	12
							−43 (Hα)	3.0	3.49	14
										13
S164	114.0 − 1.6	23^{h}35^{m}8 / 59°42'				13^{m}54	−44 (Hα)	5.1	3.43 ± 0.37	14
S165	114.61 ± 0.23	23^{h}37^{m}4 / 61°39'				12^{m}03	−27 (Hα)	2.5	2.17 ± 0.36	13, 14
							−33 (CO)	1.6 ± 0.5		12
						CO clouds				
'Large cloud'	110.5 + 2	23^{h}00^m / 62°	5 × 2°				−6 − −12		~1	25
	111 + 0		~2°5							
B12	108.03 − 0.18	22^{h}49^{m}00^s / 58°54'	12'				−38 − −60 −50			26 12
B13	108.1 − 0.50	22^{h}50^{m}19^s / 58°45'	15'				−13			12
B14	109.05 − 0.33	23^{h}00^{m}00^s / 59°12'	70'				−47			12

B15	$109.99 - 0.08$	$23^h02^m39^s$ $59°48'$	$0.5'$	-52	12
B16	$110.03 + 0.29$	$23^h01^m42^s$ $60°08'$	1.5	-52	12
B17	$110.2 + 0.21$	$23^h03^m49^s$ $59°59'$	$0.5'$	-51	12
B18	$110.24 + 0.16$	$23^h04^m10^s$ $60°00'$	$1'$	-53	12
	$111.4 + 0.9$	$23^h09^m54^s$ $61°13.9$		$-56, -14$	25
	$111.4 + 0.7$	$23^h10^m39^s$ $61°06.9$		-54	25
	$111.4 + 0.5$	$23^h11^m28^s$ $60°53.9$		-49	25
	$111.5 + 0.7$	$23^h10^m36^s$ $61°08.5$		$-57, -49$	23
	$111.5 + 0.7$	$23^h11^m28^s$ $61°31.9$		-54	23
	$111.5 + 0.8$	$23^h10^m48^s$ $61°13.5$		-57	23
	$111.5 + 0.8$	$23^h11^m22^s$ $61°13.8$		-54	23
	$111.5 + 0.8$	$23^h11^m24^s$ $61°12.8$		-57	23
	$111.5 + 0.8$	$23^h11^m37^s$ $61°11.8$		-57	23
	$111.6 + 0.9$	$23^h10^m36^s$ $61°18.5$		-54	23
	$111.6 + 0.8$	$23^h12^m12^s$ $61°13.5$		-54	23
	$111.6 + 0.8$	$23^h12^m13^s$ $61°13.9$		$-53, -11$	23
	$111.7 + 0.7$	$23^h12^m53^s$ $61°13.9$		$-50, -10$	23
	$111.7 + 0.7$	$23^h13^m53^s$ $61°08.9$		$-49, -11$	23
	$111.7 - 2.1$	$23^h21^m05^s$ $58°34.1$		$-43, 0$	23

Table III (continued)

Object	l^{II}, b^{II}	α, δ (1950)	θ	E_{B-V}	A_V	$(m-M)_0$	V_{LSR} km s^{-1}	r (kpc) Photometric	r (kpc) Kinematic	References
1	2	3	4	5	6	7	8	9	10	11
	111.7 − 2.1	23^{h}21^{m}07^s 58°32′.8					−42, −1			23
	111.7 − 2.2	23^{h}21^{m}15^s 58°31′.1					−43, −1			23
	111.8 − 2.2	23^{h}21^{m}40^s 58°31′.1					−46, 0			23
	111.8 + 0.7	23^{h}12^{m}33^s 61°13′.9					−48, −11			23
	111.9 + 0.5	23^{h}15^{m}00^s 61°05′.0					−52			23
						SNR				
Cas A	111.73 − 2.13	23^{h}21^{m}10^s +58°32′.4	4″.3		3^m–5^m		absorption −0.2, −0.6 (H$_2$CO)		2.8	27
							−36.8, −46.5, −40 (H$_2$CO)		(see text)	28
							~0 −2			29
							−40 − 47			30
							(C$_{427\alpha}$−C$_{732\alpha}$) 0, −38 − 41,			31
							−47 − −50 (HI)			32

(1) Humphreys, 1978; (2) Fenkart and Schröder, 1985; (3) Gordon et al., 1968; (4) Hoag et al., 1961; (5) Becker and Fenkart, 1971; (6) Hagen, 1970; (7) Janes and Adler, 1982; (8) Crampton, 1975; (9) Hidayat et al., 1982; (10) Grubissisch, 1965; (11) Israel et al., 1973; (12) Blitz et al., 1982; (13) Georgelin and Georgelin, 1970; (14) Georgelin et al., 1973; (15) Turner, 1979; (16) Doroshenko, 1973; (17) Israel, 1978; (18) Pedlar, 1980; (19) Deharveng, 1974; (20) Courtès et al., 1966; (21) Miller, 1968; (22) Reifenstein et al., 1970; (23) Wilson et al., 1974; (24) Hiltner, 1956; (25) Sargent, 1977; (26) Cohen et al., 1980; (27) De Jager et al., 1978; (28) Bartla et al., 1983; (29) Ershov et al., 1984; (30) Konovalenko, 1984; (31) Greisen, 1973; (32) van den Bergh, 1983.

Table III presents the summarized estimates of colour excess $E(B - V)$, absorption A_V, distance modulus, radial velocity V_{LSR} (enclosed in parentheses are lines used for measuring velocity), corresponding distances and relevant references for all emission and absorbing gas clouds, stars and stellar aggregates located in the sky region under investigation. The immediate attention is drawn by a substantial spread of the distances (from 100 pc to 6 kpc) accounted for by the fact that the line-of-sight in this direction intersects two spiral arms: the Local (Orion) arm and the Perseus–Cassiopeia arm. At the same time the variations of the radial velocity within one emission nebula or a molecular cloud do not go beyond the range of thermal motions and measurement errors.

As may be inferred from Table III, the majority of the values of the radial velocity of the emission nebulae and emission and absorbing molecular clouds are grouped in two ranges: from 0 to -20 km s^{-1} and from -35 to -60 km s^{-1}. (The corresponding kinematic distances in the Schmidt's circular motion model amount to 1.5–2 kpc and 4–5 kpc, respectively (Lang, 1978). Such ranges of the radial velocities are explained by the fact that the objects under consideration belong to two different spiral arms. The spiral structure can be well traced by the observations of neutral hydrogen line ($\lambda = 21$ cm) and CO emission line ($\lambda = 2.6$ mm). In the region of interest at $l = 108$ to $113°$ a complicated distribution of the H I clouds is observed. Thus, in the spectral contour of the 21-cm emission line one can see 7–8 details within the velocity range of from zero to -120 km s^{-1} (Westerhout, 1969; Tuve and Lundsager, 1973).
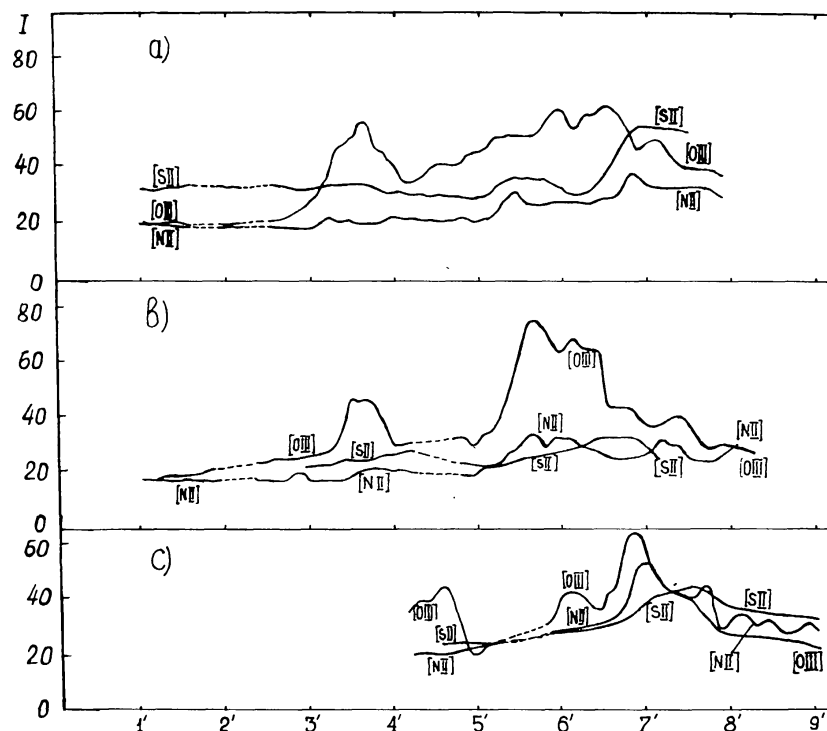
Fig. 5. Microphotometric scans of the SG 13 E: intensity versus the angular distance from the WR star HD 219460. Intensities are given in relative units different for each line.

The most prominent details in the velocity range of 0 to -20 km s^{-1} are associated with the Local spiral arm, while the range of -40 to -70 km s^{-1}, with the Perseus arm. Spiral structure of the galactic gas clouds shows up still more vividly in observations in the CO line (Cohen *et al.*, 1980). Figure 6 shows two layers of molecular clouds
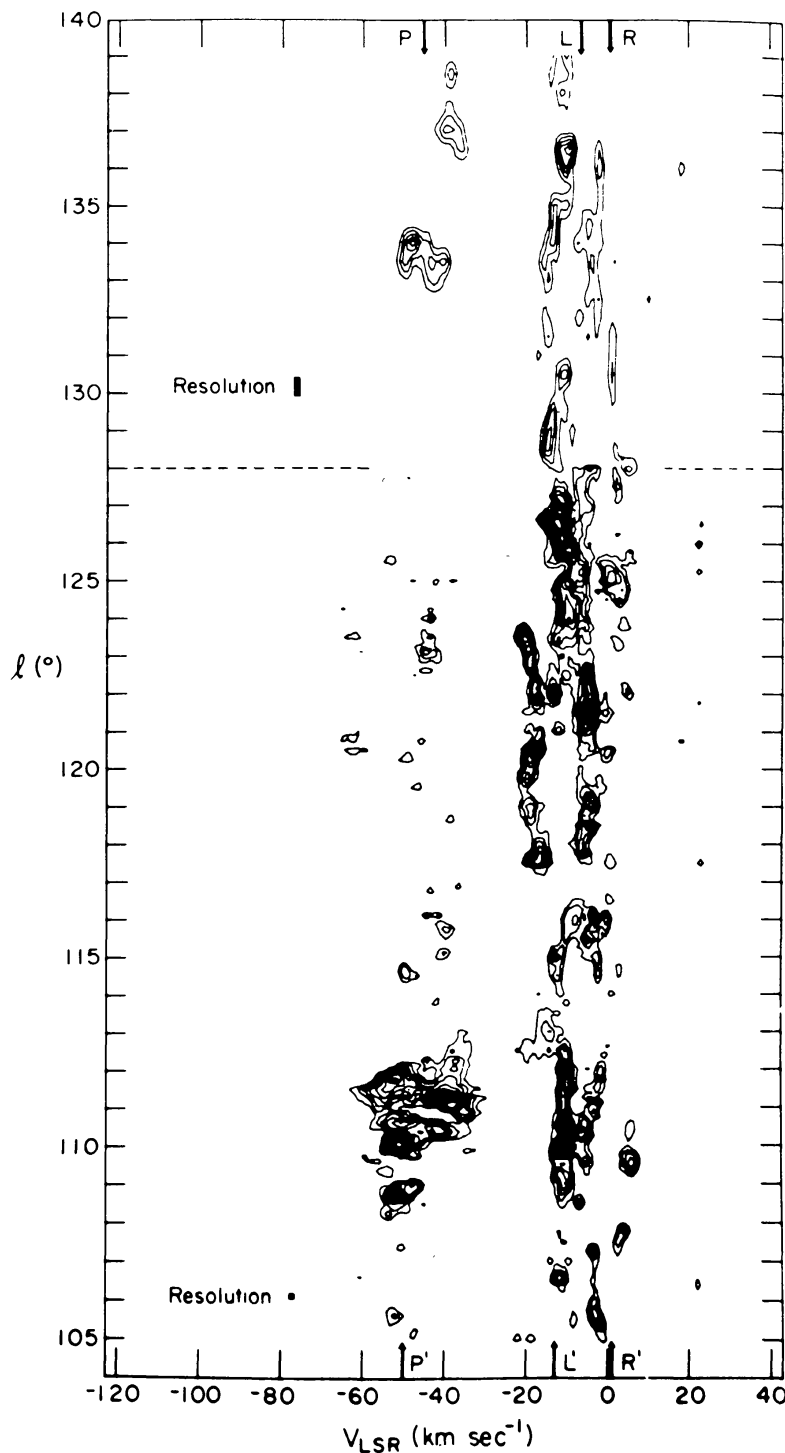

Fig. 6. Distribution of CO-brightness (galactic longitude–radial velocity diagram by Cohen *et al.*, 1980). Two layers of molecular CO-clouds are seen corresponding to the Local and Perseus spiral arms.

concentrated in the Local (V_{LSR} = 0 to -20 km s^{-1}) and Perseus (V_{LSR} = -40 to -60 km s^{-1}) arms, with the interarm space being absolutely void of clouds. The most conspicuous detail in the figure is a large molecular cloud in the region l = 110°–112°5 at a velocity of V_{LSR} = -30 to -60 km s^{-1}.

For relating the radial velocities of the molecular clouds to the distances concerned use may be made of the results of radio observations of supernova remnant Cas A. In the direction of the radiosource Cas A we can see the absorption details of numerous spectral lines (H1, OH, H$_2$CO, C$_{427\alpha}$–C$_{732\alpha}$ and so on) at the velocities of 0 to -2 km s^{-1} and -37 to -47 km s^{-1} (see Table III). At a velocity less than -50 km s^{-1} no absorption takes place, and we may ascribe the supernova distance of 2.8 kpc to this limit velocity of -48 to -50 km s^{-1}.

Comparison of the velocities of the absorption details in the direction to Cas A with the distribution of the velocity in the large molecular cloud shown in Figure 6 (l = 109–112°5, V_{LSR} = -30 to -60 km s^{-1}) makes it possible to conclude that the absorption is caused by individual gas clumps belonging to the said cloud. On the basis of this assumption we shall take the distance to the molecular cloud to be R = 2.8$^{+0.2}_{-0.4}$ kpc.

Such a distance is quite consistent with the estimates of the photometric distances to association Cas OB2 ($r \simeq$ 2.6 kpc) and to the cluster NGC 7510 ($r \simeq$ 2.9–3.1 kpc, V_{LSR} = -49 km s^{-1}). Cluster Ba 3 and WR star HD 219 460 ($r \simeq$ 1.9–2.5 kpc) as well as their surrounding nebula S157 (V_{LSR} = -33 to -55 km s^{-1}) are likely to belong to the same complex of gas, dust, and stars (see Section 6) but are located on the near boundary of the large molecular cloud.

Judging from the similar values of the radial velocities (V_{LSR} = -36 to -61 km s^{-1}) and distance moduli 12^{m}0–13^{m}5, the Perseus arm also includes: emission nebulae S156, S157A, S158, S159, S161B, S162, NGC 7635, S163, S164, S165 probably excited by the Cas OB2 stars; emission nebulae S146, S147, S148, S149, S152, S153 not more than 100 pc distant from the supposed boundary of Cas OB2 in the visual plane, numerous small-scale CO clouds located in the vicinity of the emission nebulae under discussion; and, lastly, CO-clouds B12, B14, B15, B16, B17, B18, and others registered in the lists of Blitz *et al.* (1982) and Wilson *et al.* (1974) (see Table III).

Along with these 'distant' clouds in the Perseus arm there are many clouds of gas and dust concentrated in a close circumsolar region and in the Local arm. Among them, first of all, is a dense absorbing cloud in the region of 108.5 $\leq l \leq$ 113°, 1 $\leq b \leq$ 2.5° associated with Ceph OB3 which is finely discernible in Figure 1. Judging by the radial velocity of CO line it is approximately 1 kpc distant. Related also to the Local spiral arm are clusters Ba 2 and NGC 7654, as well as a number of the OB stars and H II regions excited by them, that is corroborated by the photometric estimates of the distances to the stars and the velocity of the nebulae and obscuring clouds. Here also at a distance of $\simeq$ 1 kpc is located the neutral hydrogen shell GS 111 + 3 (Heiles, 1979).

Photometric studies of reddening of background stars in this direction also reveal the concentration of obscuring matter in two regions: nearby the Sun and in a cloud of some 1.5–2 kpc distant (Neckel and Klare, 1980). The absorption in the more distant

molecular complex in the Perseus arm is not similarly prominent apparently on account of a negligible quantity of distant stars.

To give a complete picture it is found necessary to touch upon the distant envelope H I GS 117 – 07, $\sim 8°$ in size, at the velocity $V_{LSR} = -63$ to -71 km s^{-1} (about 6 kpc distant) (Heiles, 1979) and the near Loop II (Cetus Arc) which is a shell of about 200 pc in dimension located at a distance of some 100 pc from the Sun, considered to be probably an old supernova remnant, both objects being projected on the same sector of the sky. Thus, the emission nebulae, OB stars and stellar clusters exciting them, dust and the molecular clouds in the sky region of interest exhibit a manifest tendency to concentration at the Local spiral arm (about 1 kpc) and Perseus–Cassiopeia arm (2.5–3 kpc). The latter incorporates a huge cluster of molecular clouds, dust, and stars most likely constituting a single star complex (see Section 6) to which the nebula Sh157 considered in this paper belongs.

It should be emphasized that though the mean distance to the complex of stars and nebulae in the Perseus arm has been determined with a fairly high degree of reliability, the accuracy of localization of the individual objects within the arm is not better than $\pm (200-500)$ pc.

4. Origin of the Nebula Sh157

The distinctive ring-like structure of the bright nebula SG 13 and availability of a source of strong stellar wind enable us to presume that the shell in question is essentially a product of wind from the WR star sweeping the interstellar medium. With the determined distance approximating 2.5 kpc (taking into consideration the remarks made above concerning a relatively low accuracy) the linear dimension of the bright ring nebula SG 13 corresponds to 22 × 40 pc. Taking the mean nebula density $n_e \simeq 60-100$ cm^{-3} as derived by the observations (see Section 2.1) and the visible thickness of the shell $\Delta R \simeq (0.1-0.2)$, $R \simeq 3$ pc (see Section 2.2) we can find the mass of the ionized gas: $M \simeq 300-500 \, M_\odot$. The mass of the gas that could be ionized by cluster Ba 3 (excitation parameter $U_{sp} \simeq 25-90$ for a star Wolf–Rayet and five B stars) may reach $200 \le M_{ion} \le 10^3 \, M_\odot$. Therefore, it is believed that the ring nebula SG 13 is not surrounded with an external H I layer which is formed at the late stage of development of a wind-blown bubble. Supposing the thin ionized envelope includes all the gas swept out of the full volume inside SG 13, we can find the density of undisturbed ambient gas: $n_0 \simeq 1-2$ cm^{-3}.

Taking the stellar wind power typical for stars Wolf–Rayet to be $L_W \simeq 1.3 \times 10^{37}$ erg s^{-1} ($\dot{M} = 10^{-5} \, M_\odot$ yr^{-1}, $V_\infty = 2000$ km s^{-1}) at $n_0 \simeq 1-2$ cm^{-3} for the bubble with a radius $R \simeq 15$ pc we can determine the sought duration of the stellar wind ($t_w \simeq 2 \times 10^5$ yr) and the expected velocity of the shell expansion $V_{exp} \sim 50$ km s^{-1} (Table IV), provided that the bubble is in the expansion stage with conservation of energy (model of Weaver et al., 1977). If the shell is in the expansion stage with conservation of momentum (model of Steigman et al., 1975) at the mass loss

TABLE IV

Shells formed by winds of WN 4.5 (HD 219460), Ba 3, NGC 7510, and Cas OB2

Stellar aggregate	Angular size of shell	Mean radius at $r = 2.6$ kpc	L_w (erg s^{-1})	t (10^6 yr)	
				$n_0 = 1$ cm^{-3}	$n_0 = 10$ cm^{-3}
Emission shells					
WR (SG 13)	$1 \times 0°7$	15 pc	1.3×10^{37}	0.2	
Ba 3					1–1.3
(exceed for WR)	$1 \times 1°$	20 pc	$(1–2) \times 10^{36}$	0.4–0.5	
Dust shells					
NGC 7510	$2 \times 3°$	60 pc	4×10^{36}	2.2	4.8
Cas OB2	$4 \times 5°$	113 pc	$5 \times 10^{37}–10^{38}$	2.2–2.8	4.7–6.0

rate typical for stars WR the sought wind duration will be given by

$$t_w = r^2(3\dot{M}V_\infty/2\pi\rho_0)^{-1/2} \simeq (4–5) \times 10^5 \text{ yr} .$$

The bubble age derived in both the models agrees with the duration of the strong wind of stars Wolf–Rayet, namely $t_{WR} \simeq (2–5) \times 10^5$ yr. The width of Hα line in the nebula SG 13 (FWHM $\Delta V = 44$ km s^{-1} as measured by Doroshenko, 1973) and the spread of the radial velocities of the line maximum (see Table III) is not inconsistent with our estimate of the expected expansion velocity, if the geometric projection in a thin envelope taken into account.

Consequently, the power of the wind of the star WR in terms of both the models proves to be sufficient for producing the thin envelope SG 13.

The prolate shape of the wind-blown bubble may result from nonisotropic distribution of ambient density and/or from a strong regular interstellar magnetic field in the neighbourhood of the star. Indeed, the interstellar gas is blown out much more easily in the direction of a lower density and/or along magnetic force lines. Also the regular structure of the envelope may be disturbed and broken due to instability of radiative cooling mainly along magnetic lines (Falle, 1975). For analysis of a possible effect of the magnetic field, with the purpose of revealing large-scale structure of the field in the vicinity of S157, we considered the data on polarisation radio observations of extra-galactic radio sources, pulsars, synchrotron galactic radio emission (Simard-Normadin et al., 1982) and the data obtained from optical observations of background stars light polarization at different distances from the Sun.

The prevalent direction of the magnetic field in the Local and Perseus spiral arms coincides with the direction of the galactic plane. According to the existing data, local disturbance of the field at the required distance $R \simeq 2.5$ kpc, which could explain the prolate shape of the ring nebula in the perpendicular direction, has not been revealed as yet. Some large-scale distortion of the regular structure of the galactic magnetic field was found at these galactic longitudes, but it is related to the near-circumsolar region, and is most likely associated with Loop II (Spoelstra, 1972).

Inhomogeneous distribution of the initial density in the neighbourhood of Ba 3 may result from localization of the cluster on the edge of a dense cloud or nearby the boundary of a bubble blown out by the wind of older stars (see below). An increased ambient density in the eastern part of the envelope supplies, of course, an explanation for eccentrical position of the most powerful wind source in the ring nebula – the star Wolf–Rayet. With regard to the relationship $R \propto n_0^{-(0.2 \div 0.25)}$ for expansion with concervation of energy or moment, the observed difference between the 'eastern' and 'western' radii of the envelope, i.e., $R_E/R_W \sim 0.5$, corresponds to the density contrast $n_{0E}/n_{0W} \simeq 15$–30.

The predominant mechanism of the nebula emission is photoionization by UV radiation of the central WR star and other B-stars of the cluster. This fact is attested to by the data of our observations: on the one hand, a relative intensity of lines [S II] : Hα and [N II] : Hα representative of a normal H II regions (see Section 2.2) and, on the other hand, stratification of emission in the high- and low-excitation lines (Section 2.3) opposite to that observed in supernova remnants where optical radiation is fully related to a shock wave. The UV radiation of the cluster stars, as was stated above, suffices to ionize the entire gas swept out by the stellar wind.

The similar picture is really observed in the overwhelming majority of ring nebulae around sources of strong stellar wind: i.e., the wind produce the shell-like structure of the H II region, however, the main source of ionizing radiation in the envelope is the central OB star (or stars). In the southern part of the nebula Sh157-diffuse SG 14 region – there are additional possibly exciting stars of which these two stars: Hi 1202 (B0III) and Hi 1208 (B05V) belong to the association Cas OB2 (Humphreys, 1979).

If optical emission of the nebula results from ionizing radiation of central WR star and Ba 3 stars a higher brightness of the SG 13 E region, as compared to the western part SG 13 W, is attributed to dilution of UV radiation. Since $(R_W/R_E)^2 \sim 4$, the brightness of SG 13 W according to our observations in lines [O III] and [N II] should lie within 17–20 relative units in Figure 3: i.e., it would be approximately equal to night sky brightness.

When discussing the origin of the bright shell-like nebula SG 13 around cluster Ba 3 containing binary (WR + B0III) star, we took into consideration only the wind of the latter. Really, the mass loss rates of star WR is by one order or more exceed the total stellar wind of the remaining stars in the cluster. During the past $(3$–$5) \times 10^5$ yr (the characteristic lifetime of the star in WR stage) the WR stellar wind has been predominating.

Nevertheless, the mass loss of the cluster B-stars although is relatively weak, continues for a comparatively long time. Besides, during the lifetime of the cluster ($t \simeq 10^7$ yr) probably there were other powerful but short-lived sources of stellar wind. Under the action of the Ba 3 stellar wind at the stage preceding the strong wind of star WR a shell nebula could have also be formed up. It is not inconceviable that its traces can be observed. On the photographs of S157 in lines Hα and [N II] attention is attracted by a double structure of the ring nebula: beyond the bright filaments of SG 13 one can see faint external filaments at a distance of about 20–25 pc from Ba 3 oriented

similar to the bright inner shell. The estimates given in Table IV indicate that such an envelope could be formed by B stars of the cluster Ba 3 within the time not exceeding the cluster age. The value of the integral wind power L_W is taken to be in agreement with a great number of observations of mass loss of spectral-type stars similar to the Ba 3 stars. For the value of the undisturbed gas density refer to Section 5.

5. Dust Shells Around Cluster NGC 7510 and Association Cas OB2

On the blue and red Palomar maps in the sky sector under investigation one can see not only the above-mentioned emission envelopes but also dust shells around the cluster NGC 7510 and the association Cas OB2 $\sim 3° \times 2°$ and $\sim 5° \times 4°$ in size, respectively (Figures 1 and 7). It is felt that the said shells are not only projected on Cas OB2 and NGC 7510 but also coincide with the stellar aggregates in space, since in some areas of the dust shells a CO emission is observed at velocities corresponding to the distance of 2.5 ± 0.5 kpc. What is more, the stars of the association Cas OB2 located in the region of the dust shells (see Figure 7) systematically show a greater interstellar
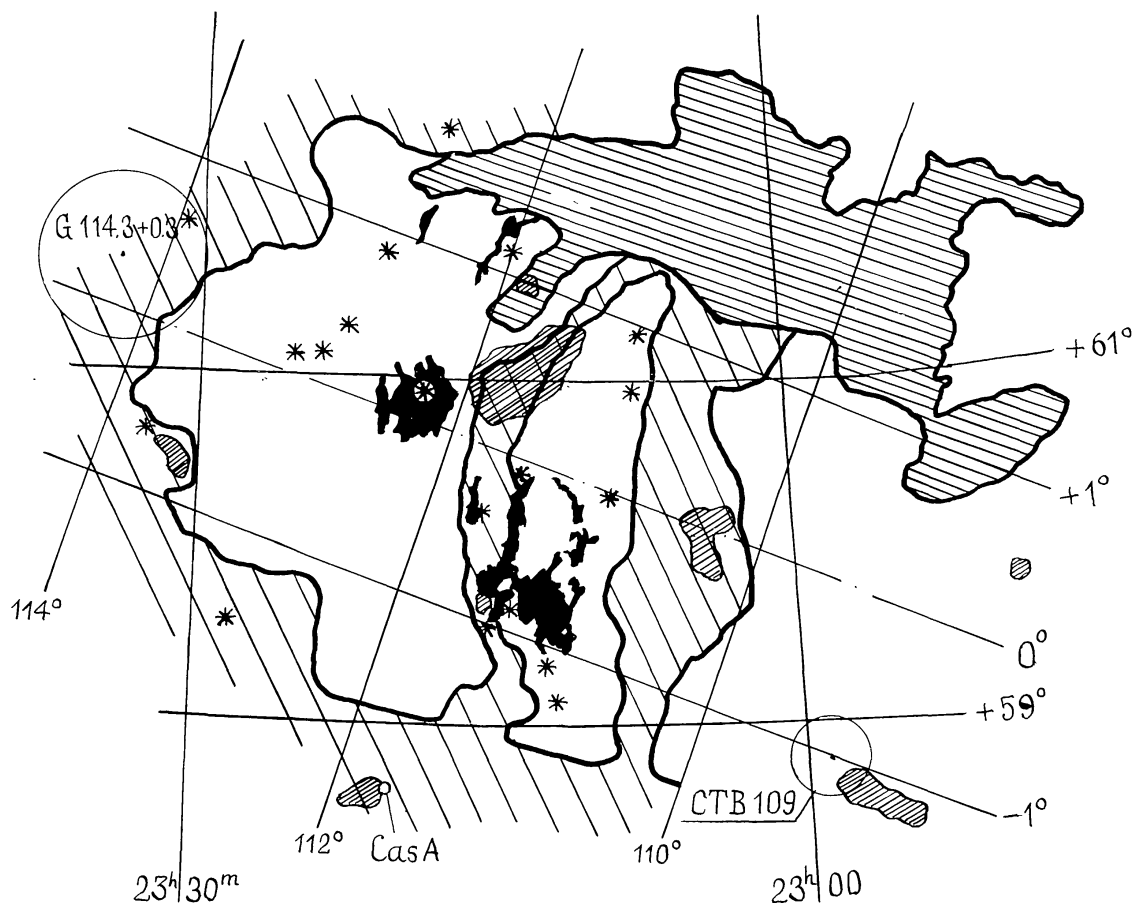
Fig. 7. Scheme of gas-dust shells in the region under consideration: ∫, H II regions; dust shells; CO emission; the nearby CO cloud; *, Cas OB2 stars.

absorption ($A_V \sim 3^m$) as compared with central stars ($A_V \sim 1\overset{m}{.}8$) according to the data obtained by Humphreys (1978), that, in all probability, bears withness to availability of dust at the periphery of the association and cluster.

It should be noted beforehand that the described dust envelopes are far less distinct than the ring nebula S157. Nevertheless we can make a rough estimate of whether the mentioned ring-shaped dust structures arose as a consequence of sweeping of interstellar gas by stellar wind of respective star aggregates. The results of this estimate are presented in Table IV.

The approximate value of the undisturbed gas density $n_0 \simeq 3$–$7 \, \text{cm}^{-3}$ is derived from the mean light absorption $\Delta A_V \sim 0\overset{m}{.}51$–$1\overset{m}{.}23$ per 100 pc in the line-of-sight inside the association. The 21-cm observations in absorption in the direction of Cas A and in emission in region $l \sim 109$–$112°$ give us the value of the density inside the spiral arm: $n_0 \simeq 10$–$50 \, \text{cm}^{-3}$ (Greisen, 1973). The results of the calculations for $n_0 = 1$ and $10 \, \text{cm}^{-3}$ are given in the appended table with due regard for the roughness of these estimates and probable local variations of the density. As an estimate of the total power of the winds of the star aggregates (L_W) we adopted certain values for the stars of different classes included in NGC 7510 (Raznik, 1965) and Cas OB2 in compliance with the catalogue of Humphreys (1979), using the data of numerous observations of mass-loss rates during the past few years, provided the said values are representative for the stars of the respective luminosity class and spectral type. As will be seen from Table IV the total wind of NGC 7510 and Cas OB2 stars seems to be capable of forming up the shells resembling the observed ones for the time not exceeding the age of these star aggregates (Section 6).

The large age of the envelopes accounts for the fact that they fail to be observed in emission. The analysis carried out by Weaver *et al.* (1977) disclosed that a wind-blown bubble at the late stage shall mainly comprise a neutral gas and dust. The entire mass of the wind-blown envelope around Cas OB2 reaches $M = (3$–$10) \times 10^5 \, M_\odot$, that consists with the typical masses of giant molecular clouds.

It should be stressed that all the estimates mentioned in this Section of the paper are tentative. As a matter of fact the mass loss rate varies from star to star within one spectral class and luminosity class, and the wind power attributed to the clusters is highly uncertain. Moreover, the formulae applied for the estimates hold true for the central point source of stellar wind, whereas the size of association Cas OB2 is comparable with that of the dust envelope. What is more, the three envelopes under consideration are distinguished arbitrarily to a large extent and therefore their reality should be confirmed by special observations. Considered to be most promising are observations in lines H I (21 cm) and CO (2.6 mm) in different ranges of velocity, that will allow to reveal the effect of expansion of the shells and to localize them in space to a higher degree of accuracy.

Should the existence of these three envelopes be corroborated, it will be interesting to find out whether or not they are physically connected, or, contrary to this, their apparent position 'one in another' is just an effect of projection.

Particularly, it is of importance to know if the asymmetry of the SG 13 envelope with

respect to Ba 3 (see Section 4) can be ascribed to inhomogeneous distribution of the ambient density due to localization of Ba 3 and star WR close to the inner boundary of the bubble blown out by the wind from NGC 7510.

6. Star Complex in the Perseus Arm

According to the up-to-date concepts the young clusters and associations are originated within star complexes of 0.5–1 kpc and over in size. The star aggregates are characterized with a hierarchic structure, i.e., several clusters and associations make up a 'group', two-three groups unite into star complexes which form up spiral arms in S-galaxies (see Efremov, 1984; and associated references *ibid.*).

By the time of formation of a cluster the most part of the mass of the parent molecular cloud remains unlost, therefore the process of star formation continues in it. The new burst of star formation is initiated by expansion of ionization fronts and shock waves caused by stellar winds and supernovae. This 'active' phase of evolution of a molecular complex lasts for a period of 10^7–10^8 yr which is comparable with lifetime of massive stars and star clusters and associations; however, this exceeds considerably the time of condensation of stars from a protostellar cloud and also the time of dissipation of supernova remnants and bubbles blown by a strong wind of an individual star. That is why we can observe genetically related star clusters and associations, giant H II complexes and molecular clouds, expanding shells and supershells, formed by stellar wind of OB-associations and by numerous supernova explosions, regions of star formation on their boundaries, as well as small-scale ring nebulae – remnants of last supernovae and bubbles around individual stars with strong winds. This is probably the case of such a genetically relationship of different populations of a star complex that is observed in the Perseus arm region under consideration.

The clusters Ba 3, NGC 7510 and the association Cas OB2 constitute a single group, judging by near localization in space and similar age. It is not improbable that the associations Cas OB1, OB2, OB4, OB5, OB7, OB8, and Ceph OB1, OB5 located in the near region of the Perseus arm make up the subsequent hierarchic cell – a giant star complex. A large-scale structure of the stellar aggregates, associated H II regions, dust clouds and supernova remnants is depicted in Figure 8. The association boundaries are shown according to Humphreys (1978). Table V indicates the age of the clusters determined by the position of the Main-Sequence turn-off point. The age of the associations was determined by the absolute magnitudes of the brightest blue stars and Main Sequence stars (Hodge, 1983) on the basis of the data listed by Humphreys (1978). As may be seen from Table V the above-listed star aggregates in the Perseus arm are similar in age, that makes it possible to suppose their simultaneous formation, most likely as a result of passing the spiral density waves.

It is also possible that the cepheid complex Cas C4 revealed by Efremov (1978) also belongs to the same stellar aggregate. This cepheid group is located in the sector of the sky $111 \le l \le 118°$, $-3 \le b \le +1°$ and is limited to $2.8 \le r \le 3.6$ kpc in distance.

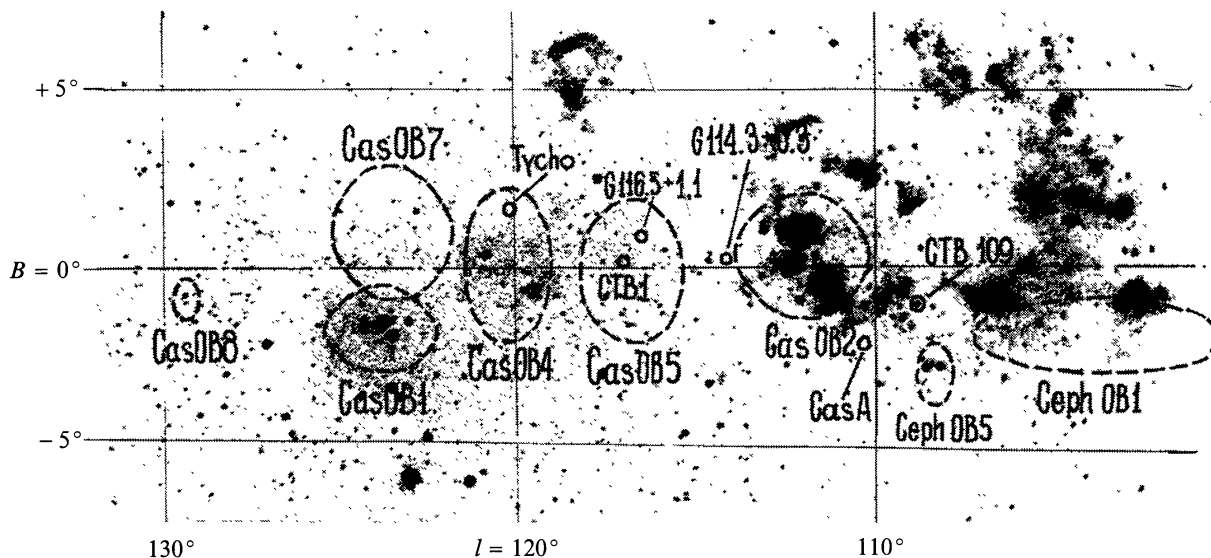It should be emphasized that this is independent estimate of the distance (by the

Fig. 8. OB-associations (dash line) and supernova remnants in Perseus arm; superimposed on the mosaic (Hα + [N II]) photographs by Dubout-Crillon (1976).

period-luminosity relationship of the Cepheids) and it is as accurate as 10%. The given distance limits are determined by extreme periods of the Cepheids in the group.

The extreme values of the radial velocities of the cepheid complex members: $-56 \le V_{LSR} \le -77$ km s^{-1} roughly coincide with the radial velocity of the large molecular cloud in the sector $110 \le l \le 112.5°$. The distance to the Cepheids and gas-dust fragments of this cloud are also similar. The difference between the velocities of the large gas cloud and Cas C4 probably reflects the initial motions of fragments of a giant protostellar molecular complex.

If Cepheid group Cas C4 is genetically related to the large molecular cloud and star aggregate composed of Cas OB2, Ba 3, and NGC 7510, then the dispersion of the complex members ages determined by the extreme periods of the Cepheids corresponds to $(1-7) \times 10^7$ yr.

Probably, it should be unreasonable to neglect the following rather speculative scheme: Cas OB2 stellar wind formed a dust shell during the period of $t_w \sim (2-5) \times 10^6$ yr (see Table IV). After the next 5×10^6 yr (the minimum estimate of NGC 7510 age, see Table V) the cluster NGC 7510 arose whose wind in turn produced a bubble. On the edge of the latter the emission shell S157 was formed by the stellar wind of WR star for the time of approximately $(2-5) \times 10^5$ yr. Such a cascading process of star formation is quite possible, though as concerns NGC 7510 formation after Cas OB2 we have no evidence of its applicability, for even the estimates of age of the objects are far from being certain. (The WR star is naturally the youngest one.) The above-mentioned asymmetrical position of star WR HD 219460 and the cluster NGC 7510 in their shells probably may serve as some indirect argument in favour of this hypothesis.

TABLE V

Stellar aggregate, limiting l, b	R (kpc)	M_V max, Main Sequence	t_1 (years)	M_V max, blue	t_2 (years)	Accepted age
1	2	3	4	5	6	7
Cep OB1 100–108° −3−−1°	3.47	$-5\overset{m}{.}1$	4×10^6	$-7\overset{m}{.}5$	8×10^6	6×10^6
NGC 7235 102°7 0°8	4.07			$-6\overset{m}{.}7$	10^7	10^7
Cep OB5 108.3–108°6 −3.2−−2°3	2.9	$-3\overset{m}{.}8$	10^7			10^7
Cas OB2 110.1–114°0 −1.3−1°8	2.6	$-3\overset{m}{.}4$	10^7	$-7\overset{m}{.}2$	9×10^6	10^7
Cas OB5 115–118° −2.4−1°3	2.51	$-4\overset{m}{.}3$	8×10^6	$-7\overset{m}{.}4$	9×10^6	8×10^6
Cas OB4 119.0–121°6 −2.1−2°0	2.88	$-4\overset{m}{.}8$	6×10^6	$-6\overset{m}{.}2$	10^7	8×10^6
Cas OB7 121.7–125°2 −0.9−2°6	2.51	$-4\overset{m}{.}3$	8×10^6	$-7\overset{m}{.}2$	9×10^6	8×10^6
Cas OB1 122.3–125°8 −2.3−−0°4	2.51			$-5\overset{m}{.}9$	10^7	10^7
Cas OB8 129.2–129°7 −1.5−−0°2	2.88	–		–		–
NGC 7510						5×10^6–8×10^7
Ba 3						8×10^6–2×10^7
Cas C4 111–118° −3−+1°	2.8–3.6					10^7–7×10^7

Table V contains the following information (in order of columns): (1) star aggregation and its limiting l and b; (2) distance; (3) absolute magnitude of youngest star in the Main Sequences; (4) respective age; (5) absolute magnitude of brightest blue star; (6) respective age; (7) accepted average age. The age of clusters NGC 7510 and Ba 3 is determined by the Main-Sequence turn-off point. The dispersion of the Cas C4 age is derived on the basis of the limiting values of the cepheid periods.

The age of the clusters and associations under consideration is sufficiently large for completing the evolution of their most massive members. Therefore, it is believed that the supernova remnants (for their parameters see Table VI) observed in the region of interest are formed as a result of explosions of the stars contained in this aggregates. The supernova progenitors are most likely to belong to associations Cas OB2 and Cep OB1 containing many massive stars of early-spectral classes. This undoubtedly applies to the Cas A because of the mass and chemical composition of the supernova ejecta give evidence for rather high initial mass of the progenitor: i.e., $M_{\text{init}} \gtrsim 20\text{--}25\,M_\odot$ (see, for example, Markert *et al.*, 1983).

TABLE VI

Supernova remnants in star complex

Name	l, b (deg)	Angular dimension (arc min)	V_{LSR} (H I, Hα) (km s^{-1})	r		Age (years)	References
				Kinematic (kpc)	$\Sigma(D)$ (kpc) (5)		
CTB 109	109.2 − 1.0	32			5–6	1600	3
Cas A	111.7 − 2.1	3	0 − − 50 (abs)	2.8	calibrating source	300	2, 3
	114.3 + 0.3	66	− 35 − − 45	3.4 ± 0.4	4.0	3×10^5	1
	116.5 + 1.1	62	− 45 − − 65	4.4 ± 0.8	3.1	3×10^5	1
CTB 1	116.9 + 0.2	26	− 35 − − 50	3.4 ± 0.6	6	3×10^4	2, 1
Tycho	120.09 + 1.4	8	8 − − 50 (abs)	∼3	4	400	4

Based on the data derived by: (1) Reich, Braunfurth, 1981; (2) Lozinskaya, 1981; (3) Hughes *et al.*, 1983; (4) Henbest, 1980; (5) Milne, 1979.

The initial mass of the stars which have produced the old supernova remnants CTB 1, G114.3 + 0.3, and G116.5 + 1.1 is unknown. Therefore, our assumption of probable genetically relationship between them and nearby located OB-associations is based only on general ideas concerned with supernova rate in associations (1 SN for $(1\text{--}5) \times 10^5$ yr) as well as the lifetime of an association ($\sim 10^7$ yr) and the time of dissipation of supernova remnants ($5 \times 10^4\text{--}10^5$ yr), but has not proved in any way. Object CTB 109 containing a compact stellar remnant of a supernova explosion, as was demonstrated by the observations of Fahlman and Gregory (1983), is most likely to originate in a low-massive binary system. With an initial mass $M_{\text{init}} \leq (1\text{--}3)\,M_\odot$ the lifetime of the system proves to exceed the age of the association, and the object is unlikely to be genetically related to young stars of the OB-associations.

The star aggregate including Ba 3, NGC 7510, and Cas OB2 additionally contains a fairly rich reserve of material of the parent molecular complex. The large molecular cloud in the direction $l = 109\text{--}112°$, that was discussed above in Section 3, consists at least of three large fragments spaced apart and rather different in velocity (see Figure 6). Observations in radio lines of highly excited carbon, formaldehyde and in other

molecular lines mentioned in Section 3 are indicative of a high density $(n_H \sim 10^3\text{--}10^4 \text{ cm}^{-3})$ in small-scale molecular condensations of some 0.1–0.01 pc in size (Bartla *et al.*, 1983). Judging by the radial velocity of the condensations the latter should belong to this massive molecular cloud (see Section 3). Besides separate dense molecular clouds identified by emission or absorption in the CO line, as well as dust clusters and H I clouds are scattered all over the Perseus arm region of interest.

This region also contains sources of external dynamics pressure – potential triggers of gravitational instability inducing a new star formation process in the molecular complex. These are, primarily, extensive expanding shells around Ba 3, NGC 7510, and Cas OB2 which were spoken of in Sections 4 and 5. It is precisely the boundary of such shells and supershells given rise to by radiation, several supernovae and stellar winds of OB associations, but not in shells of individual supernovae, where regions of star formation are usually observed. In future, in the course of expansion and overlaping with other shells the aforesaid supernova remnants and bubbles blown by winds of individual stars, SG 13, NGC 7635 and the like will probably become star-formation triggers.

The process of star formation in the molecular complex is being in progress. Located in the southern section of nebula S157 are the well-known compact source S157 A, probably a cocoon star S157 B, two greatly reddened compact H II regions (Israel *et al.*, 1973) and dense compact CO condensations (Israel, 1978); the other cocoon star is S158 G near the nebula S158.

It should be noted that the star formation regions are observed precisely where interstellar medium is disturbed 'twice': on the boundary of the expanding NGC 7510 wind-blown bubble and of the expanding H II region SG 13.

Thus, the region of interest shows all signs of a single young star aggregate comprising: two clusters and OB-association of similar age; complex of H II regions; giant molecular cloud with continuing star formation process; remnants of supernovae likely belonging to the association; bubbles and 'superbubbles' blown out by winds of individual stars, clusters, and OB-associations.
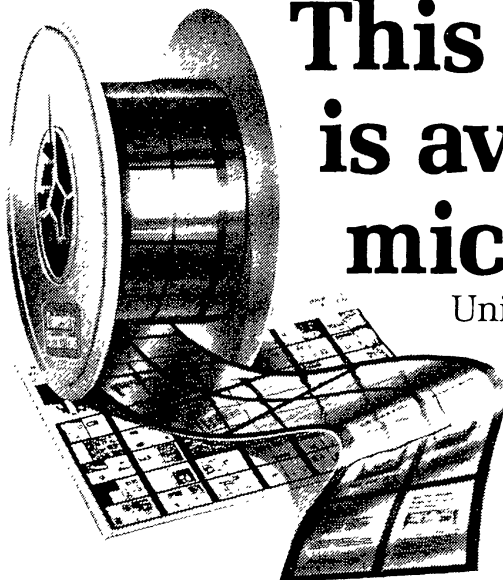
Acknowledgements

References

Bartla, W., Wilson, T. L., and Martin-Pintado, J.: 1983, *Astron. Astrophys.* **119**, 139.
Becker, W., Muller, E., and Stenlin, U.: 1955, *Z. Astrophys.* **38**, 81.
Becker, W. and Fenkart, R.: 1971, *Astron. Astrophys. Suppl. Ser.* **4**, 241.
Blitz, L., Fich, M., and Stark, A. A.: 1982, *Astrophys. J. Suppl. Ser.* **49**, 183.
Broten, N. W., Macleod, J. M., and Vallee, J. P.: 1985, *Astrophys. Letters* **24**, 165.
Chopinet, M. and Lortet-Zuckerman, M. C.: 1972, *Astron. Astrophys.* **18**, 373.
Chopinet, M. and Lortet-Zuckerman, M. C.: 1976, *Astron. Astrophys. Suppl. Ser.* **25**, 179.
Cohen, R. S., Cong, H., Dame, T. M., and Thaddeus, P.: 1980, *Astrophys. J.* **239**, L53.

Courtès, G., Cruvellier, P., and Georgelin, Y.: 1966, *Observatory* **49**, 329.

Crampton, D.: 1975, *Publ. Astron. Soc. Pacific* **87**, 523.

Deharveng, L.: 1974, *Astron. Astrophys.* **35**, 63.

De Jager, G., Graham, D. A., Wielebinski, R., Booth, R. S., and Gruber, G. M.: 1978, *Astron. Astrophys.* **64**, 17.

Doroshenko, V. T.: 1973, Thesis, Moscow University, Moscow.

Dubout-Crillon, R.: 1976, *Astron. Astrophys. Suppl. Ser.* **25**, 25.

Efremov, Yu.: 1978, *Pis'ma Astron. Zh.* **4**, 125.

Efremov, Yu.: 1984, *Vestn. Akad. Nauk.* **12**, 56.

Ershov, A. A., Ilyasov, Yu. P., Lekht, E. E., Smirnov, A. T., Solodkov, V. T., and Sorochenko, R. L.: 1984, *Pis'ma Astron. Zh.* **10**, 833.

Fahlman, G. G. and Gregory, P. C.: 1983, in J. Danzinger and P. Gorenstein (eds.), 'Supernova Remnants and Their X-Ray Emission', *IAU Symp.* **101**, 445.

Falle, S. A. E. G.: 1975, *Astron. Astrophys.* **43**, 323.

Fenkart, R. P. and Schröder, A.: 1985, *Astron. Astrophys. Suppl. Ser.* **59**, 83.

Gaze, V. Ph. and Shain, G. A.: 1955, *Izv. Krymsk. Astrophys. Obs.* **15**, 11.

Georgelin, Y. P.: 1970, *Astron. Astrophys.* **7**, 322.

Georgelin, Y. P. and Georgelin, Y. M.: 1970, *Astron. Astrophys.* **6**, 349.

Georgelin, Y. M., Georgelin, Y. P., and Roux, S.: 1973, *Astron. Astrophys.* **25**, 377.

Gershberg, R. E. and Metik, L. P.: 1960, *Izv. Krymsk. Astrophys. Obs.* **24**, 148.

Glyshkov, Ju. L., Eroshevich, A. S., and Karyakina, Z. V.: 1972, *Trudy Astrophys. Inst. Alma-Ata* **19**, 79.

Gordon, C. P., Howard, III, W. E., and Westerhout, C.: 1968, *Astrophys. J.* **154**, 103.

Greisen, E. W.: 1973, *Astrophys. J.* **184**, 363.

Grubissisch, C.: 1965, *Z. Astrophys.* **60**, 256.

Hagen, G. L.: 1970, *Publ. David Dunlap Obs.* **4**, 1.

Heckathorn, J. H., Bruhweiler, F. G., and Gull, T. R.: 1982, *Astrophys. J.* **252**, 230.

Heiles, C.: 1979, *Astrophys. J.* **229**, 533.

Henbest, S. N.: 1980, *Monthly Notices Roy. Astron. Soc.* **190**, 833.

Hidayat, B., Supelli, K., and van der Hucht, K. A.: 1982, in C. W. H. de Loore and A. J. Willis (eds.), 'WR Stars: Observations, Physics, Evolution', *IAU Symp.* **99**, 27.

Hiltner, W. A.: 1956, *Astrophys. J. Suppl. Ser. 2* **24**, 389.

Hoag, A. A., Johnson, H. L., Iriarte, N., Mitchell, R. J., Hallam, K. L., and Sharpless, S.: 1961, *Publ. U. S. Naval Obs. Ser.* **2**, 17, 7.

Hodge, P. W.: 1983, *Astrophys. J.* **264**, 470.

Hughes, V. A., Harten, R. H., Costain, C. H., Nelson, L. A., and Viner, M. R.: 1984, *Astrophys. J.* **283**, 147.

Humphreys, R. M.: 1970, *Astron. J.* **75**, 602.

Humphreys, R. M.: 1978, *Astrophys. J. Suppl. Ser.* **38**, 309.

Israel, F. P.: 1978, *Astron. Astrophys.* **70**, 769.

Israel, F. P., Habing, H. J., and de Long, T.: 1973, *Astron. Astrophys.* **27**, 143.

Janes, K. and Adler, D.: 1982, *Astrophys. J. Suppl. Ser.* **49**, 425.

Kamper, K. W. and Van den Bergh, S.: 1983, in J. Danziger and P. Gorenstein (eds.), 'Supernovae and Their X-Ray Emission', *IAU Symp.* **101**, 55.

Konovalenko, A. A.: 1984, *Pis'ma Astron. Zh.* **10**, 846.

Lang, K. R.: 1978, *Astrophysical Formulae*, Springer-Verlag, Berlin.

Lomovski, A. I. and Klement'eva, A. Yu.: 1985, *Astron. Zh.* (in press).

Lozinskaya, T. A.: 1981, *Pis'ma Astron. Zh.* **7**, 29.

Lozinskaya, T. A., Sitnik, T. A., Toropova, M. S., and Klement'eva, A. Yu.: 1984, *Pis'ma Astron. Zh.* **10**, 122.

Lozinskaya, T. A., Sitnik, T. A., and Toropova, M. S.: 1986, *Astron. Zh.* (in press).

Lindoff, U.: 1968, *Arkiv Astron. Stockholm* **5**, 1.

Markarian, B. E.: 1951, *Soobshch. Byurakan. Obs. Akad. Nauk Arm.. S.S.R.* **9**, 7, 39.

Markert, T. H., Canizares, C. R., Clark, G. W., and Winkler, R. F.: 1983, *Astrophys. J.* **268**, 134.

Miller, J. S.: 1968, *Astrophys. J.* **151**, 473.

Milne, D. K.: 1979, *Australian J. Phys.* **32**, 83.

Neckel, Th. and Klare, G.: 1980, *Astron. Astrophys. Suppl. Ser.* **42**, 251.

Nosov, I. V.: 1979, *Soviet Astron. Tsirc.* **1050**, 1.

Pedlar, A.: 1980, *Monthly Notices Roy. Astron. Soc.* **192**, 179.

Raznik, R. M.: 1965, *Izv. Krymsk. Astrophys. Obs.* **24**, 148.

Reich, W. and Brausfurth, E.: 1981, *Astron. Astrophys.* **99**, 17.

Reinfenstein, E. C., Wilson, T. L., Burke, B. F., Mezger, P. G., and Altenhoff, W. J.: 1970, *Astron. Astrophys.* **4**, 357.

Sakhibov, Ph. H.: 1980, *Pis'ma Astron. Zh.* **6**, 101.

Shain, A. A., and Gaze, V. Ph.: 1951, *Izv. Krymsk. Astrophys. Obs.* **12**, 93.

Simard-Normandin, M., Kronberg, P. P., and Button, S.: 1982, *Astron. Astrophys. Suppl.* **48**, 137.

Sitnik, T. G. and Toropova, M. S.: 1982, *Pis'ma Astron. Zh.* **8**, 679.

Sitnik, T. G., Klement'eva, A. Yu., and Toropova, M. S.: 1983, *Astron. Zh.* **60**, 503.

Sharpless, S.: 1959, *Astrophys. J. Suppl. Ser.* **4**, 257.

Spoelstra, T. A. T.; 1972, *Astron. Astrophys.* **21**, 61.

Steigman, G., Strittmater, P. A., and Williams, R. E.: 1975, *Astrophys. J.* **198**, 575.

Turner, B. E.: 1979, *Astron. Astrophys. Suppl. Ser.* **37**, 1.

Tuve, M. A. and Lundsager, S.: 1973, *A Sky Atlas of Neutral Hydrogen Emission*, Carnegie Inst., Washington, No. 630.

Van den Bergh, S.: 1983, in J. Danziger and P. Gorenstein (eds.), 'Supernova Remnants and Their X-Ray Emission', *IAU Symp.* **101**, 597.

Weaver, R., McCray, R., Castor, J., Shapiro, P., and More, R.: 1977, *Astrophys. J.* **218**, 377.

Westerhout, G.: 1969, *Maryland-Green Bank Galactic 21-cm Line Survey* (second edition).

Wilson, W. J., Schwartz, R. P., Epsteine, E. E., Johnson, W. A., Etcheverry, R. D., Mori, T. T., Berry, A. A., and Dyson, H. B.: 1974, *Astrophys. J.* **191**, 357.